Metal-poor Molecular Gas in Edge Cloud 2

P. M. E. Ruffle[1]* T. J. Millar[1] H. Roberts[1] D. A. Lubowich[2] C. Henkel[3] G. Brammer[4] J. M. Pasachoff[4]

[1]The University of Manchester, UK [2]Hofstra University, USA [3]Max-Planck Institut für Radioastronomie, Germany [4]Williams College, USA *Email: paul.ruffle@manchester.ac.uk*

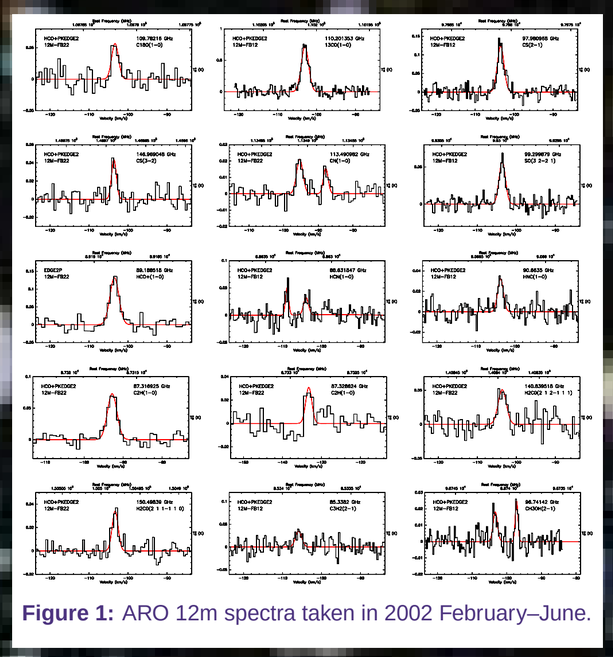

Figure 1: ARO 12m spectra taken in 2002 February–June.

Observations of CO emission at large Galactocentric distances have detected a number of molecular clouds (Digel et al. 1994), including Edge Cloud 2 (EC2) at a kinematic galactocentric distance of 28 kpc, some 8 kpc further away than the next most distant molecular cloud, and much further than the extent of the optical disk of the Milky Way, ∼ 19 kpc, and almost as far as the most distant H I detected, at ∼ 30 kpc. EC2 has an effective radius of 20 pc, and is situated some 360 pc below the distant warped Galactic plane (Digel et al. 1996a). The CO maps of EC2 show that it has sub-structure and that the CO luminosity of EC2 is at least a factor of 2 larger than those ofthe other 10 clouds detected in the survey by Digel et al., and comparable to that of the Taurus Giant Molecular Cloud.

EC2 was found to have an associated H II region excited by an early B star MR1 (de Geus et al. 1993). Kobayashi & Tokunaga (2000) used NIR observations to argue that MR1 has triggered the formation of young stellar objects in EC2, and Snell et al. (2002) argue that it is the most distant star-forming cloud in the Milky Way, with evidence for massive star formation. Rolleston et al. (2000) have calculated metal depletion for C, N, O ∼ 5, and EC2 is the only edge cloud detected in the high-density tracer CS (Digel et al. 1996b). Studies of metallicity as a function of galactocentric distance have shown that there is a galactic gradient and that spectra of MR1 by Smartt et al. (1996) indicate significant metal depletion, with elemental abundances reduced on average by some 0.5 dex.

Because EC2 may represent a local example of low-metallicity gas, with properties similar to those of irregular dwarf galaxies, we have searched for emission from a number of molecules in order to constrain physical conditions and chemical composition.

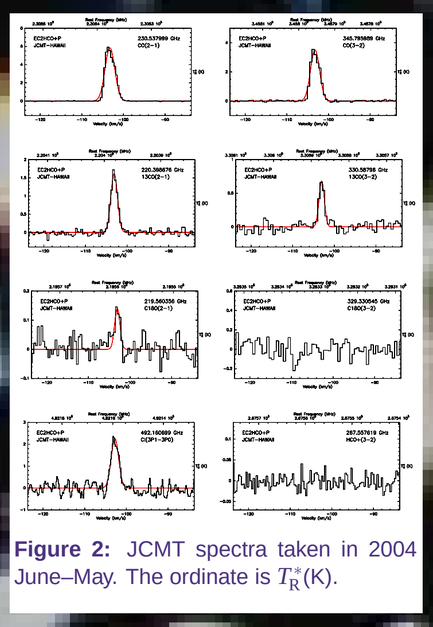

Figure 2: JCMT spectra taken in 2004 June–May. The ordinate is T_R^*(K).

Observations

We have observed EC2 using the ARO 12m, the MPIfR 100m, and the JCMT 15m telescopes. The observations range in frequency from 4.83 GHz (H_2CO $1_{1,1}$–$1_{1,2}$) to 492 GHz (C I $^3P_1$–$^3P_0$). We present results for position A at $\alpha_{1950} = 02^h44^m52.6^s$, $\delta_{1950} = 58°16'00''$, which shows the strongest line spectrum. Figures 1, 2 & 3 show the lines detected and Table 1 summarises our observational data.

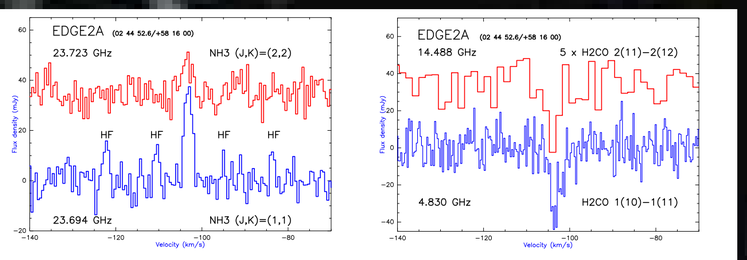

Figure 3: NH_3 (J,K) = (1,1) and (2,2) spectra (left) and H_2CO $2_{11} - 2_{12}$ and $1_{10} - 1_{11}$ (right) observed with the MPIfR Effelsberg 100m radio telescope.

Analysis

We have detected a total of 12 hyperfine lines of NH_3. Deriving a rotational temperature of T = 20±3 K, the total NH_3 column density, becomes N(NH_3) = 5.72×10^{12} cm^{-2} ±20%, averaged over our 40″ beam. We used this rotational temperature to estimate the density through two approaches: The first was to use H_2CO for which the peak line intensity ratio is of the order of 5. Assuming that the cloud is optically thin in both lines and extended, we derive a spatial density of about 5×10^4 cm^{-3} (Henkel et al. 1980). In addition, we made some Large Velocity Gradient (LVG) models and found that n(H_2) = 5×10^3 cm^{-3} gave the best fit to both the absorption and emission lines. The second approach was to fit the ^{13}CO and C^{18}O spectra to an LVG model using collisional rates from Flower (2001) and an adopted ortho-para ratio of 3 for H_2. Since the 2–1 transitions are stronger than the 1–0 and 3–2 transitions, we find that the density is $\sim 5 \times 10^3$ cm^{-3}. Our best fit gives a fractional abundance of $\sim 10^{-8}$ for ^{13}CO, substantially below the value of 2×10^{-6} typically found in local metal-rich molecular clouds.

In order to derive accurate molecular abundances one needs multiple transitions of a variety of isotopomers to account for optical depth and excitation effects. Furthermore, the use of optically thin transitions is also fraught with difficulty since the underlying isotopic ratios may be different at the edge of the Galaxy than in more local molecular clouds. For species other than CO, H_2CO and NH_3, we have assumed LTE and an excitation temperature of 20 K. Since most of the derived abundances are not very sensitive to temperature, we present results for the latter case only. Table 1 lists the derived column densities.

To aid comparison with local molecular clouds, we have derived molecular abundances relative to that of HCO^+, assuming that the 1–0 transition is optically thin. Our upper limit to $H^{13}CO^+$ gives a lower limit to $HCO^+/H^{13}CO^+$ of around 9, much less than the lower limit of 201±15 derived from CO 1–0 by Wouterloot & Brand (1996) towards WB 89-437 at a galactocentric distance of 16.4 kpc. Table 2 shows the result and also the equivalent abundance ratio for the nearby dark clouds L134N and TMC-1 (Dickens et al. 2000; Pratap et al. 1997).

Discussion

Current models include time and spatial variations in the infall and star formation rate whereby the Galactic halo, bulge, and thick disk formed first separately from the thin disk in two infall episodes. Chemical abundances of the interstellar medium and their radial variation across galactic disks provide a fundamental set of constraints for theories of disk formation and evolution. The most accepted mechanism to explain the existence of abundance gradients in disk galaxies is the so called 'biased-infall' (Chiappini & Matteucci 1999), where infall of gas occurs at a faster rate in the innermost regions than in the outermost ones. Lubowich et al. (2000) demonstrated that continuous infall of low-metallicity gas is continuously occurring in the Galactic Center.

Of particular relevance to testing these models are the abundances in the very outer galactic disks. Chemical evolution models for abundance gradients and the formation of the Milky Way (Chiappini et al. 2001) show that the steepness of the outer gradients are particularly sensitive to thresholds in star formation, to the halo-thick disk enrichment history, and to the radial variation of the disk formation timescales. The fact that N is almost constant with galactocentric distance up to 18 kpc (Chiappini et al. 2003) reflects the high N production in AGB stars. Galactic chemical evolution also predict that the abundances of C, N, O, ^{13}C, and ^{15}N will be the lower at the edge than in any other interstellar cloud (Maciel & Quireza 1999). The composition of these clouds should be similar to that of the early Galactic disk modified by infall from the halo. Thus the metallicity is expected to be lower and similar to dwarf irregular galaxies, giving us an unique opportunity to study gas from the early stages of the formation of the Galactic disk (Kobayashi & Tokunaga 2000). Our results will determine early Galactic abundances, test models of Galactic chemical evolution, and provide important information that will constrain nucleosynthesis, chemical evolution, and astrochemistry models. If there is any gradient in the N abundance beyond 18 kpc, then there would be evidence that this cloud has not had significant AGB or massive star formation. Thus EC2 has not had significant stellar processing during the past 10 Gyr and is a remnant of the gas that formed the Galactic disk.

Molecule	Transition	Freq. (GHz)	T_R^*	ΔV (km s^{-1})	rms (K)	N (cm^{-2})
CO[a]	1–0	115.271	5.90	2.77	0.075	$1.87 \pm 0.16\ 10^{16}$
C^{18}O	1–0	109.782	0.057	2.05	0.014	$1.48 \pm 0.44\ 10^{14}$
^{13}CO	1–0	110.201	0.718	2.23	0.065	$1.81 \pm 0.21\ 10^{15}$
^{13}CO[a]	1–0	110.201	1.110	2.03	0.049	$2.55 \pm 0.22\ 10^{15}$
C^{17}O	1–0	112.359	—	—	0.007	$<3.21\ 10^{13}$
C^{18}O	2–1	219.560	0.142	1.48	0.031	$1.13\ 10^{14}$
^{13}CO	2–1	220.399	1.608	1.87	0.069	$1.61\ 10^{15}$
CO	2–1	230.538	5.843	2.76	0.024	$8.16\ 10^{15}$
C^{18}O	3–2	329.330	—	—	0.020	$<3.65\ 10^{13}$
^{13}CO	3–2	330.588	0.649	1.69	0.025	$5.76\ 10^{14}$
CO	3–2	345.796	3.467	2.56	0.019	$4.58\ 10^{15}$
C I	$^3P_1$–$^3P_0$	492.161	2.358	2.23	0.398	$7.17\ 10^{16}$
CS	2–1	97.981	0.125	2.18	0.013	$1.55 \pm 0.20\ 10^{12}$
CS	3–2	146.969	0.043	1.46	0.008	$2.27 \pm 0.55\ 10^{11}$
C^{34}S	3–2	144.617	—	—	0.010	$<1.21\ 10^{11}$
CN	$1,\frac{3}{2},\frac{3}{2}$–$0,\frac{1}{2},\frac{1}{2}$	113.488	0.016	1.71	0.004	$1.15 \pm 0.41\ 10^{12}$
CN	$1,\frac{3}{2},\frac{5}{2}$–$0,\frac{1}{2},\frac{3}{2}$	113.491	0.021	2.22	0.004	
SO	1_0–0_1	30.002	0.073	1.50	0.018	$1.21\ 10^{13}$
SO	3_2–2_1	99.300	0.057	1.93	0.007	$8.52 \pm 1.29\ 10^{12}$
DCO^+	1–0	72.039	—	—	0.005	$<5.20\ 10^{10}$
$H^{13}CO^+$	1–0	86.754	—	—	0.009	$<6.11\ 10^{10}$
HCO^+	1–0	89.189	0.132	2.73	0.014	$5.42 \pm 0.80\ 10^{11}$
HCO^+	3–2	267.558	—	—	0.012	$<1.60\ 10^{10}$
$H^{13}CN$	1–0	86.340	—	—	0.006	$<7.00\ 10^{10}$
HCN	1–0	88.632	0.036	1.51	0.013	$1.40 \pm 0.59\ 10^{11}$
HCN		88.634	0.051	1.03	0.013	
HNC	1–0	90.664	0.032	1.40	0.007	$1.06 \pm 0.38\ 10^{11}$
C_2H	1–0	87.317	0.073	2.87	0.007	$1.87 \pm 0.25\ 10^{13}$
C_2H		87.329	0.031	1.86	0.007	
N_2H^+	1–0	93.174	—	—	0.007	$<5.29\ 10^{10}$
H_2CO	$1_{1,0}$–$1_{1,1}$	4.830	-0.028	3.2	0.006	$2.46 \pm 0.66\ 10^{12}$
H_2CO	$2_{1,1}$–$2_{1,2}$	14.488	-0.011	1.3	0.006	
H_2CO	$2_{1,2}$–$1_{1,1}$	140.840	0.051	2.51	0.013	
H_2CO	$2_{1,1}$–$1_{1,0}$	150.498	0.034	1.77	0.005	
NH_3	1–1	23.694	0.040	2.0	0.006	$5.72 \pm 1.15\ 10^{12}$
NH_3	2-2	23.723	0.015	2.6	0.005	
HC_3N	9–8	81.881	—	—	0.007	$< 1.40\ 10^{11}$
C_3H_2	$2_{1,2}$–$1_{0,1}$	85.338	0.035	1.92	0.016	
CH_3OH	2_{-1}–1_{-1} E	96.739	0.025	0.97	0.005	
CH_3OH	2_0–1_0 A^+	96.741	0.019	1.37	0.005	

[a]Data taken with the ARO 12m 2005 February.

Table 1: Summary of observations toward EC2 position A. Column densities are estimated for an excitation temperature of 20K.

The data in Table 2 indicate some interesting differences between EC2 and local molecular clouds. In particular: sulphur-bearing molecules, (CS, SO), appear to be very over-abundant; the nitrogen-bearing species HCN and HNC appear to be marginally under-abundant; and the radicals CN and C_2H are very much over-abundant. The latter result is typical of photon-dominated regions in which photoprocesses ensure that radicals exist in high abundance. At first glance it would appear that the molecular clouds at the edge of the Galaxy would be less likely to show the effects of PDR chemistry; certainly the flux of UV photons must be much less at 28 kpc than in the local ISM. However, the critical parameter for determining whether or not photons dominate chemistry is the ratio of UV flux to grain surface area. At large galactocentric radii, the metal abundances relative to hydrogen are expected to be much reduced as discussed above. In addition, although the region of EC2 does contain young stars (de Geus et al. 1993), there is no evidence of the late-type stars which produce dust grains. The large abundances of NH_3 and SO also indicate that the chemical evolution is fairly highly evolved, that is, more indicative of steady-state rather than early-time chemistry. To investigate the properties of the cloud and to see whether it is typical of material which has been less processed, we have made a chemical kinetic model using our observationally derived temperatures and densities, varying elemental abundances, photon fluxes and gas-to-dust ratios in an attempt to fit our observed results.

X/HCO^+	T_x = 20 K	L134N	TMC-1	L134N range	EC2/H2	TRANS/H2
CO 1-0[h]	34500	11000[b]	7800[b]		1.9-7	
^{13}CO 1-0	3339	172[a]	122[a]	111-188	1.8-8	
^{13}CO 1-0[h]	4698	172[a]	122[a]	111-188	2.6-8	
C^{18}O 1-0	273	22.00	15.60	14.2-24	1.4-9	
C^{17}O 1-0	<59.3	—	—		<3.2-10	
^{13}CO 2-1	2970	172[a]	122[a]		1.6-8	
C^{18}O 2-1	209	22.00	15.60		1.2-9	
CO 2-1	27887	11000[b]	7800[b]		8.2-8	
^{13}CO 3-2	1063	172[a]	122[a]		5.8-9	
C^{18}O 3-2	<67.3	22.00	15.60		1.2-9	
CO 3-2	8450	11000[b]	7800[b]		4.6-8	
C I	$1.29\ 10^5$	—	—		7-7	
CS 2-1	2.86	0.124	0.320	0.069-0.138	1.6-11	1.1-8
CS 3-2	0.42	0.124	0.320		2.3-12	
C^{34}S 3-2	< 0.22	—	—		<1.2-12	
DCO^+ 1-0	<0.10	—	—		< 5.2-13	
$H^{13}CO^+$ 1-0	<0.11	[c]	[c]		<6-13	
$H^{13}CN$ 1-0	<0.13	[c]	[c]		<7-13	
CN[d]	2.12	0.061	0.070	<0.045-0.069	1.2-11	
HCN 1-0	0.26	0.925	0.490	0.555-0.968	1.4-12	3.6-8
HNC 1-0	0.20	3.251	1.680	1.324-3.963	1.0-12	2.5-9
C_2H 1-0[e]	34.9	0.288	0.300	0.171-0.333	1.9-10	6.6-8
N_2H^+ 1-0	<0.10	0.077	0.013	0.031-0.077	<5.3-13	1-9
HC_3N	<0.26	0.054	0.150	0.030-0.073	<1.4-12	5-10
NH_3	10.6	7.635	2.770	4.284-9.127	5.7-11	2.1-8
H_2CO	4.54				2.5-11	6.3-9
CH_3OH		0.641	0.099	0.311-0.641		1.8-8
SO[f]	22.3	0.719	0.130	0.264-0.738	1.2-10	3.2-8
SO[g]	15.7	0.719	0.130	0.264-0.738	8.5-11	

[a] ^{13}CO/C^{18}O ratio of 7.81 assumed. [b] ^{12}CO/C^{18}O ratio of 500 assumed. [c] ^{12}C/^{13}C ratio of 64 assumed. [d]From the sum of the two components assuming a relative intensity of 0.456. [e]From the 87.317 GHz component assuming a relative intensity of 0.4167. [f]From the 30 GHz line. [g]From the 99.3 GHz line. [h]Data taken with the ARO 12m 2005 Feb.

Table 2: Molecular abundances ratios relative to HCO^+ in both EC2, L134N (center position) and TMC-1 (average) (Dickens et al. 2000). Using numbers derived at the JCMT; optically thin emission assumed for all; no isotopic ratio corrections. N(HCO^+) = 5.42 10^{11} cm^{-2} for T_x = 20 K. N(H_2) = 10^{23} cm^{-2} assumed in calculation of the EC2 fractional abundances, so that X(HCO^+) = 5.4 10^{-12}. TRANS/H2 from translucent cloud observations by Turner (2000)

Chemical Modelling

The basic model assumes T_{kin} = 20K, n(H_2) = 5×10^3 cm^{-3}, based on our NH_3, H_2CO, and CO observations, and for metals C, N, O, S, initial elemental abundances reduced by a factor of five from those typically used for local clouds. We have also investigated varying the cosmic ray ionisation (CRI) rate and the visual extinction (A_V) in order to try and find the best fit to the observations. To test the agreement between each model and the observations we looked at the ratio of the observed abundance to the model prediction and applied a weighting factor for each molecule/transition.

We investigated the agreement factor at steady state ($t > 10^6$ yr) for values of A_V between 2 and 10 mag, and a CRI rate between 0.5 and 20 times the standard interstellar rate of 1.3×10^{-17} s^{-1} Although many of the models give very similar results, the agreement factor is highest for a CRI rate 20× the ISM value and an A_V of 3 mag. Model 1 uses 'standard' ISM values for the A_V and CRI rate, Model 2 is the 'best fit' model (CRI=2.6×10^{-16} s^{-1}, A_V = 3 mag), while Model 3 uses CRI=1.3×10^{-16} s^{-1} and A_V = 2 mag. We have assumed that the isotopic ratios (e.g. ^{13}C/^{12}C) have their local interstellar values.

We have also looked at the effect of varying the photon field in the models. At steady-state CO is primarily destroyed by photons (if the UV field is strong enough, or the A_V low enough) or by He^+ and H_3^+, whose abundances increase with increasing CRI rate. The predicted DCO^+/HCO^+ ratio is 0.1–0.2 in these models, similar to the observed upper limit. Cosmic ray ionisation of H_2 and He produce electrons which can destroy H_3^+ before it can react with HD, the initial step to deuterating most molecular ions. The C_2H/HCO^+ and CN/HCO^+ ratios both decrease as the A_V increases, which means that the A_V = 2 mag model is good for C_2H, but that the A_V = 3 and 5 mag models are better for CN. Finally, we note that there is a much better fit to the ammonia abundance in all three of these low-UV models while HNC is also closer to its observed value.

References

Chiappini, C. & Matteucci, F. 1999, Ap&SS, 265, 425
Chiappini, C., Matteucci, F., & Romano, D. 2001, ApJ, 554, 1044
Chiappini, C., Romano, D., & Matteucci, F. 2003, MNRAS, 339, 63
de Geus, E. J., Vogel, S. N., Digel, S. W., & Gruendl, R. A. 1993, ApJL, 413, L97
Dickens, J. E., Irvine, W. M., Snell, R. L., et al. 2000, ApJ, 542, 870
Digel, S., de Geus, E., & Thaddeus, P. 1994, ApJ, 422, 92
Digel, S. W., Hunter, S. D., Mukherjee, R., et al. 1996a, in IAU Symp. 170: CO: 25 Years of mm-Wave Spectroscopy, 22–+
Digel, S. W., Lyder, D. A., Philbrick, A. J., Puche, D., & Thaddeus, P. 1996b, ApJ, 458, 561
Flower, D. R. 2001, J. Phys. B: At. Mol. Opt. Phys., 43, 2731
Henkel, C., Walmsley, C. M., & Wilson, T. L. 1980, A&A, 82, 41
Kobayashi, N. & Tokunaga, A. T. 2000, ApJ, 532, 423
Lubowich, D. A., Pasachoff, J. M., Balonek, T. J., et al. 2000, Nature, 405, 1025
Maciel, W. J. & Quireza, C. 1999, A&A, 345, 629
Pratap, P., Dickens, J. E., Snell, R. L., et al. 1997, ApJ, 486, 862
Rolleston, W. R. J., Smartt, S. J., Dufton, P. L., & Ryans, R. S. I. 2000, A&A, 363, 537
Smartt, S. J., Dufton, P. L., & Rolleston, W. R. J. 1996, A&A, 305, 164
Snell, R. L., Carpenter, J. M., & Heyer, M. H. 2002, ApJ, 578, 229
Wouterloot, J. G. A. & Brand, J. 1996, A&AS, 119, 439

Background image: Seven red NIR (near infrared) sources associated with EC2 (Kobayashi & Tokunaga 2000). PMER acknowledges receipt of a PPARC studentship. Astrophysics at The University of Manchester is supported by PPARC. DAL thanks Hofstra University for a Faculty Research and Development Grant. Poster presented at Astrochemistry – Recent Successes and Current Challenges – IAU Symposium 231, 29 Aug - 2 Sep 2005, Asilomar, Monterey, California, USA. This poster has been typeset from a TEX / LATEX file prepared by the author.